Math. Model. Nat. Phenom.
Vol. 8, No. 6, 2013, pp. 64–79
DOI: 10.1051/mmnp/20138605

Travelling Waves in Plankton Dynamics

M. Semplice, E. Venturino *

Dipartimento di Matematica "Giuseppe Peano"
Università di Torino, Italy

Abstract. A recently proposed model for the investigation of diffusivity in planktonic systems containing toxin-producing phytoplanktons is here reconsidered. We show the existence of planktonic travelling waves. Numerical simulations validate the analytical findings, to elucidate the sensitivity of the results in dependence of the diffusion coefficients.

Keywords and phrases: competition models, food web, toxic phytoplankton, minimal models

Mathematics Subject Classification: 92D25, 92D40, 35Q92

1. Introduction

In the past quarter of century research on plankton dynamics has become relevant, both at the biological level, as well as from the modelling point of view. Plankton has indeed a paramount importance in the aquatic food webs, since it represents the lower trophic level in such chains. Mathematical models for planktonic systems including space dependence often lead to the discovery of insurgences of patterns, see the second half of [7] for an account of these topics, both from the deterministic and stochastic points of view.

A phenomenon that has negative impact on tourism and the fisheries industries is due to red tides, the sudden blooms of algae, [1, 6, 11]. Some species of phytoplankton can release poisons that affect zooplankton as well as possibly, directly or indirectly, also fish. Recent investigations have shown that movement can sustain inhomogeneous distribution levels of plankton communities composed of non-toxic phytoplankton, toxic phytoplankton and zooplankton, [3, 10]. An idea that has been proposed for explaining the insurgence of red tides is that they are side effects caused by these toxin producing phytoplanktons, [4, 5, 8, 9].

In this paper we develop further the work undertaken in [2] on diffusive plankton movements, for which the action of the toxin-producing phytoplankton not only damages the grazers, but it can also cause spatial inhomogeneities. In [2] the steady states of this plankton model have been investigated and the corresponding spatiotemporal patterns discovered. Here, we study the possible insurgence of planktonic travelling waves, that ultimately produce these steady state distributions.

*Corresponding author. E-mail: matteo.semplice@unito.it, ezio.venturino@unito.it

© EDP Sciences, 2013

https://doi.org/10.1051/mmnp/20138605 Published online by Cambridge University Press
Article published by EDP Sciences and available at http://www.mmnp-journal.org or http://dx.doi.org/10.1051/mmnp/20138605

The results show that when a new species appears at a single location in a system that is at equilibrium, it may originate an invading wave. We confirm previous findings and exhibit traveling waves that leave behind them the non spatially-uniform coexistence equilibrium of the toxic model.

The paper has the following structure. The next Section presents the model, which is analysed in Section 3. Travelling waves are investigated in Section 4 for the nontoxic model and in Section 5 for the toxic one. Then numerical simulations follow, to substantiate and extend the analytical findings. The sensitivity of the results on the diffusion coefficients is also investigated.

2. The population model

We consider a model for three interacting plankton species of the form:

$$\frac{\partial p_k}{\partial t} = f_k(\mathbf{p}) + D_k \Delta p_k, \qquad k = 1, 2, 3 \tag{2.1}$$

where Δ represents the Laplacian and $\mathbf{p}(t,x) = (p_1(t,x), p_2(t,x), p_3(t,x))$ are the densities of each population at location x in space, D_k are diffusion coefficients and the reaction terms described by f_k model the interactions among the populations. Since (2.1) represents a population model, the densities must be non-negative, $p_i(t,x) \geq 0$, $i = 1,2,3$ for $(t,x) \in \{\mathbf{R}^+ \times \mathbf{R}^+\}$, as well as the initial conditions, $p_i(0,x) = p_i^{(0)}(x)$ where the latter represent given functions.

More precisely we consider the model studied in [2] where p_1 and p_2 are phytoplankton species and p_3 reprents zooplankton that feeds on the other two. In [2] two versions of the model are considered: the case where p_2 is toxic for the zooplankton is compared to the standard situation.

$$\begin{aligned}
f_1^{(\mathrm{std})}(\mathbf{p}) = f_1^{(\mathrm{tox})}(\mathbf{p}) &= p_1 \left[r_1 \left(1 - \frac{p_1 + \psi_1 p_2}{K} \right) - \alpha_1 p_3 \right] \\
f_2^{(\mathrm{std})}(\mathbf{p}) = f_2^{(\mathrm{tox})}(\mathbf{p}) &= p_2 \left[r_2 \left(1 - \frac{p_2 + \psi_2 p_1}{K} \right) - \alpha_2 p_3 \right] \\
f_3^{(\mathrm{std})}(\mathbf{p}) &= p_3 \left(\beta p_1 - c + \delta p_2 \right) \\
f_3^{(\mathrm{tox})}(\mathbf{p}) &= p_3 \left(\beta p_1 - c - \tfrac{\theta p_2^2}{m + p_2} \right)
\end{aligned} \tag{2.2}$$

In these models it is assumed that both harmless and toxic phytoplankton live in the same environment and share common resources, for which the first two equations in (2.2) exhibit the same carrying capacity K. They do reproduce at different rates, however. Respectively, the latter are r_1 and r_2. The coefficient ψ_1 measures in a sense the competition ability of the phytoplankton p_2 over the phytoplankton population p_1, or in other words the damage that the former inflicts to the latter. A similar description holds conversely for ψ_2. The parameters α_i, $i = 1,2$ represent the grazing rates of zooplankton over each phytoplankton population. The p_1 biomass is then converted into new zooplankton via the uptake rate β. The natural zooplankton mortality is denoted by c. The last terms in the last two equations of (2.2) differ in sign, as they model two different situations. The former describes the standard situation, p_2 is converted into new zooplankton biomass at rate δ. The latter instead states that toxic phytoplankton kills the zooplankton at rate θ. In this case, also the functional form is different. In [2] the linear form has been chosen for the standard case, while the multiplier

$$\frac{p_2}{m + p_2}$$

has the form of a Holling type II response function, where m represents the half-saturation constant. Thus it tends to vanish for a small toxic phytoplankton population, while it exhibits a saturation phenomenon when the population becomes very large. Hence, the multiplier is not constant, but an implicit nonlinear function of time. The reason might be due to the fact that for the poison to be effectively released, a small number of toxic phytoplankton is not sufficient. At the same time, when the harmful phytoplanktons are

https://doi.org/10.1051/mmnp/20138605 Published online by Cambridge University Press

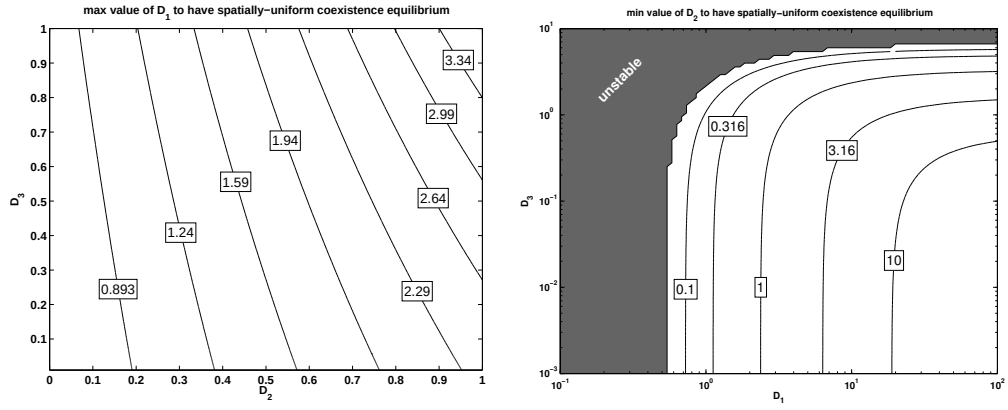


FIGURE 1. Threshold values of the diffusion coefficients for the stability of the spatially stable uniform coexistence equilibrium in the toxic model. Left: threshold for D_1 as a function D_2 and D_3. Right: threshold for D_2 as a function D_1 and D_3. In the shaded region on the right, the stable coexistence equilibrium in always non-uniform.

in large numbers, the assumption in (2.2) is that there is a maximal toxin release rate. Other options could have been simply again a linear rate or, alternatively, a Holling type II response function, for which the square in the numerator would not appear in the last equation of (2.2). Taking these models from the available literature, in this paper we investigate how the spatial configurations of these systems evolve in time, disregarding the fact that they do not contain the same functional response.

In [2] it is shown that both models admit a spatially uniform stable state corresponding to a nontrivial coexistence equilibrium of the three species, but that in the scenario where the second phytoplankton species is toxic, this is stable only if the mobility D_1 of the nontoxic prey is smaller than a threshold value that depends on the parameters in the reaction terms and on the other two diffusion coefficients. Figure 1 depicts such threshold as a function of D_2 and D_3 for the values of the parameters used in [2] and in the numerical tests of this paper (see Sec. 6)

3. Travelling waves

In this paper we concentrate on the regimes where a spatially uniform coexistence equilibrium is spatially stable, i.e. we restrict to D_1 small enough in the toxic scenario, and show that travelling wave solutions representing the invasion of the spatial domain by the p_2 species are allowed in the model.

By travelling wave solution we mean a solution of the form

$$p_k(t,x) = \hat{p}_k(x - vt) = P_k(s) \tag{3.1}$$

for some constant speed v with $\hat{p}_k$ constant away from the origin and "linking" the initial data with the stable equilibrium:

$$\lim_{\xi \to -\mathrm{sgn}(v)\cdot\infty} \hat{p}_k(\xi) = p_k^{\mathrm{eq}} \qquad \lim_{\xi \to +\mathrm{sgn}(v)\cdot\infty} \hat{p}_k(\xi) = p_k^{\mathrm{initial}}$$

Ecologically, this means that the appearence of individuals of the p_2 population, for instance, in a given domain (where p_1 and p_3 are in equilibrium) gives rise to an invasion front moving at constant speed and separating the initial state (ahead of the front) and the nontrivial equilibrium (behind the front).

On differentiating (3.1) we have

$$\frac{\partial \hat{p}_k}{\partial t} = -vP_k', \quad \frac{\partial^2 \hat{p}_k}{\partial x^2} = P_k''$$

https://doi.org/10.1051/mmnp/20138605 Published online by Cambridge University Press

We can now rewrite the first two equations in the systems in terms of the new functions P_k as follows

$$\begin{aligned} -vP_1' &= P_1\left[r_1 - \frac{r_1}{K}\left(P_1 + \psi_1 P_2\right) - \alpha_1 P_3\right] + D_1 P_1'' \\ -vP_2' &= P_2\left[r_2 - \frac{r_2}{K}\left(P_2 + \psi_2 P_1\right) - \alpha_2 P_3\right] + D_2 P_2'' \end{aligned} \tag{3.2}$$

while the third equation in the non-toxic case is

$$-vP_3' = P_3\left[\beta P_1 + \delta P_2 - c\right] + D_3 P_3'' \tag{3.3}$$

and in the toxic case instead is

$$-vP_3' = P_3\left[\beta P_1 - \frac{\theta}{m + P_2} P_2^2 - c\right] + D_3 P_3''. \tag{3.4}$$

Defining $Q_k = P_k'$ for $k = 1, 2, 3$, we obtain the systems

$$\begin{aligned} P_k' &= Q_k \\ Q_1' &= \frac{1}{D_1} P_1\left[\alpha_1 P_3 + \frac{r_1}{K}\left(P_1 + \psi_1 P_2\right) - r_1\right] - \frac{v}{D_1} Q_1 \\ Q_2' &= \frac{1}{D_2} P_2\left[\alpha_2 P_3 + \frac{r_2}{K}\left(P_2 + \psi_2 P_1\right) - r_2\right] - \frac{v}{D_2} Q_2 \\ Q_3' &= \frac{1}{D_3} P_3\left[c - \beta P_1 - \delta P_2\right] - \frac{v}{D_3} Q_3, \end{aligned} \tag{3.5}$$

in the non-toxic case and instead for the toxic case

$$\begin{aligned} P_k' &= Q_k \\ Q_1' &= \frac{1}{D_1} P_1\left[\alpha_1 P_3 + \frac{r_1}{K}\left(P_1 + \psi_1 P_2\right) - r_1\right] - \frac{v}{D_1} Q_1 \\ Q_2' &= \frac{1}{D_2} P_2\left[\alpha_2 P_3 + \frac{r_2}{K}\left(P_2 + \psi_2 P_1\right) - r_2\right] - \frac{v}{D_2} Q_2 \\ Q_3' &= \frac{1}{D_3} P_3\left[c - \beta P_1 + \frac{\theta}{m + P_2} P_2^2\right] - \frac{v}{D_3} Q_3. \end{aligned} \tag{3.6}$$

4. Waves for the non-toxic model

We investigate the equilibria of (3.5) at first. For all of them we must have $Q_k = 0$, and then seek the population levels P_k that annihilate the right hand sides of the system. Restricting just to the $P_1 - P_2 - P_3$ phase subspace, we find the points $X_0 \equiv (0, 0, 0)$, $X_1 \equiv (K, 0, 0)$, $X_2 \equiv (0, K, 0)$, always feasible,

$$X_3 \equiv \left(0, \frac{c}{\delta}, \left(1 - \frac{c}{\delta K}\right)\frac{r_2}{\alpha_2}\right), \quad X_4 \equiv \left(\frac{c}{\beta}, 0, \left(1 - \frac{c}{\beta K}\right)\frac{r_1}{\alpha_1}\right),$$

which are feasible respectively for

$$\delta K > c \tag{4.1}$$

and

$$\beta K > c. \tag{4.2}$$

We find also

$$X_5 \equiv \left(\frac{K}{\Delta}(1 - \psi_1), \frac{K}{\Delta}(1 - \psi_2), 0\right), \quad \Delta = 1 - \psi_1\psi_2$$

https://doi.org/10.1051/mmnp/20138605 Published online by Cambridge University Press

feasible when either one of the two following alternative sets of conditions holds

$$1 > \psi_1, \quad 1 > \psi_2; \quad 1 < \psi_1, \quad 1 < \psi_2. \tag{4.3}$$

In addition there is the point X_6 with all populations at nonzero levels.

The Jacobian of (3.5) in the phase space $P_1 - P_2 - P_3 - Q_1 - Q_2 - Q_3$ is a partitioned matrix in 3×3 blocks

$$J = \begin{pmatrix} O & I \\ A & B \end{pmatrix} \tag{4.4}$$

where

$$A = \begin{pmatrix} A_{11} & \frac{r_1\psi_1}{KD_1}P_1 & \frac{\alpha_1}{D_1}P_1 \\ \frac{r_2\psi_2}{KD_2}P_2 & A_{22} & \frac{\alpha_2}{D_2}P_2 \\ -\frac{\beta}{D_3}P_3 & -\frac{\delta}{D_3}P_3 & A_{33} \end{pmatrix}$$

with

$$A_{11} = \frac{1}{D_1}\left(\alpha_1 P_3 + r_1\frac{2}{K}P_1 + \frac{r_1\psi_1}{K}P_2 - r_1\right),$$
$$A_{22} = \frac{1}{D_2}\left(\alpha_2 P_3 + r_2\frac{2}{K}P_2 + \frac{r_2\psi_2}{K}P_1 - r_2\right),$$
$$A_{33} = \frac{1}{D_3}\left(c - \beta P_1 - \delta P_2\right),$$

and

$$B = \operatorname{diag}\left(-\frac{v}{D_1}, -\frac{v}{D_2}, -\frac{v}{D_3}\right).$$

Exchanging the pairs of rows and columns 2 and 4, then 4 and 6, followed by a block interchange of the last two rows and columns, and finally exchanging the rows and columns 3 and 4, the matrix $J - \lambda I$ is reduced to block form, in which each block is a 2 by 2 matrix. Its final form is as follows

$$J - \lambda I = \begin{pmatrix} -\lambda & 1 & 0 & 0 & 0 & 0 \\ A_{11} & -\frac{v}{D_1} - \lambda & A_{12} & 0 & A_{13} & 0 \\ 0 & 0 & -\lambda & 1 & 0 & 0 \\ A_{21} & 0 & A_{22} & -\frac{v}{D_2} - \lambda & A_{23} & 0 \\ 0 & 0 & 0 & 0 & -\lambda & 1 \\ A_{31} & 0 & A_{32} & 0 & A_{33} & -\frac{v}{D_3} - \lambda \end{pmatrix}.$$

This corresponds also to a rearrangement of the vector of the unknown populations, as follows: $(P_1, P_1', P_2, P_2', P_3, P_3')^T$. Although for our purposes the case of the origin is not very much interesting, we present it nevertheless, in order to better illustrate the procedure we use in the relevant cases that follow. At the origin, only the diagonal blocks in the Jacobian are nonzero,

$$J - \lambda I = \begin{pmatrix} -\lambda & 1 & & & & \\ -\frac{r_1}{D_1} & -\frac{v}{D_1} - \lambda & & & & \\ & & -\lambda & 1 & & \\ & & -\frac{r_2}{D_2} & -\frac{v}{D_2} - \lambda & & \\ & & & & -\lambda & 1 \\ & & & & \frac{c}{D_3} & -\frac{v}{D_3} - \lambda \end{pmatrix}.$$

The determinant is thus the product of the determinants of each such block, giving therefore

$$\left[\lambda\left(\frac{v}{D_3} + \lambda\right) - \frac{c}{D_3}\right] \Pi_{i=1}^{2} \left[\lambda\left(\frac{v}{D_i} + \lambda\right) + \frac{r_i}{D_i}\right] = 0$$

https://doi.org/10.1051/mmnp/20138605 Published online by Cambridge University Press

The eigenvalues are immediately readable, as roots of the quadratic equations arising from each block. For $i = 1, 2$ we have

$$D_i\lambda^2 + v\lambda + r_i = 0,$$

from which using Descartes' rule of signs, we thus find two negative roots. But from the last one, we have

$$D_3\lambda^2 + v\lambda - c = 0,$$

which instead has always a positive root. Thus we have shown the following result.

Proposition 4.1. *The origin is unstable.*

We have further:

Proposition 4.2. *X_1 and X_2 are also unstable.*

Proof. For these cases it is also easy to establish instability.

In fact for X_1 we have $A_{21} = A_{23} = A_{31} = A_{32} = 0$ and $A_{11} = r_1 D_1^{-1}$. With the same procedure we find that the Jacobian is a block upper triangular matrix, from which the eigenvalues again come from the 2×2 diagonal blocks. In particular the equation

$$D_1\lambda^2 + v\lambda - r_1 = 0,$$

by Descartes' rule has one positive eigenvalue.

At X_2 the Jacobian has the same structure as for X_1. Instead we have $A_{31} = A_{32} = A_{12} = A_{13} = 0$ and $A_{22} = r_2 D_2^{-1}$, so that this time it is the equation

$$D_2\lambda^2 + v\lambda - r_2 = 0 \tag{4.5}$$

that has a positive eigenvalue. □

Remark 4.3. These results are somewhat expected, since they show that perturbing a system with no populations or only one by adding another one, the system will thrive.

Consider now X_3.

Proposition 4.4. *X_3 is an unstable equilibrium point.*

Proof. Since $A_{12} = A_{13} = 0$, here the Jacobian factorizes and the characteristic equation is the product of a quadratic and a quartic. The former,

$$D_1\lambda^2 + v\lambda - D_1 A_{11} = 0,$$

has roots of uncertain sign, while the latter is

$$\lambda^4 + a_3\lambda^3 + a_2\lambda^2 + a_1\lambda + a_0 = 0. \tag{4.6}$$

The coefficients a_k, $k = 0, \dots 4$ are known. We provide here the most important ones: $a_0 = A_{22}A_{33} - A_{23}A_{32}$ and

$$a_3 = \frac{v}{D_2 D_3}(D_2 + D_3) > 0, \quad a_1 = -\frac{v}{D_2 D_3}(A_{22} + A_{33}) = -\frac{cr_2 v}{D_2 D_3 K\delta} < 0.$$

In view of Descartes' rule, we have at least one negative and one positive root; the latter thus provides instability. □

Proposition 4.5. *X_4 is also unstable.*

https://doi.org/10.1051/mmnp/20138605 Published online by Cambridge University Press

Proof. We find $A_{21} = A_{23} = 0$, so that from the central block of the partitioned Jacobian a quadratic characteristic equation arises, with roots of uncertain sign

$$D_2\lambda^2 + v\lambda - D_2A_{22} = 0.$$

The remaining quartic is again (4.6). Its most important coefficients are $a_0 = A_{11}A_{33} - A_{13}A_{31}$ and

$$a_3 = \frac{v}{D_1D_3}(D_1 + D_3) > 0, \quad a_1 = -\frac{v}{D_1D_3}(A_{11} + A_{33}) = -\frac{cr_1v}{D_1D_3K\beta} < 0.$$

In view of Descartes' rule, we again find at least one negative and one positive root; the latter thus provides instability. □

Proposition 4.6. *X_5 is an unstable equilibrium.*

Proof. Note that $A_{31} = A_{32} = 0$, so that again the Jacobian factorizes. The quadratic characteristic equation is now

$$D_3\lambda^2 + v\lambda - D_3A_{33} = 0.$$

but the signs of the roots are not clear. The quartic originating from the remaining part of the Jacobian is once more (4.6). Again, we provide the coefficients whose signs are known, $a_0 = A_{11}A_{22} - A_{12}A_{21}$,

$$a_3 = \frac{v}{D_1D_2}(D_1 + D_2) > 0, \quad a_1 = -\frac{v}{D_1D_2}(A_{11} + A_{22}).$$

Here, observe that the feasibility conditions (4.3) imply that $A_{11} > 0$ and $A_{22} > 0$, because we have

$$A_{11} = \frac{r_1}{D_1\Delta}(1 - \psi_1), \quad A_{22} = \frac{r_2}{D_2\Delta}(1 - \psi_2).$$

Thus $a_1 < 0$ and by Descartes' rule, there is at least one negative and one positive root, for which instability follows. □

Thus, all the boundary equilibrium points in the six-dimensional phase space are unstable, so that any trajectory leaving near them has to remain away from the coordinate hyperplanes.

To complete our analysis, we need to show that the trajectories emanating from these unstable equilibria remain in the feasible region.

Proposition 4.7. *The trajectories originating from the unstable boundary equilibria enter into the feasible orthant $\{(P_1, P_2, P_3) : P_i \geq 0, i = 1, 2, 3\}$.*

Proof. Let us consider first the origin. Let $\lambda^* > 0$ be the positive eigenvalue, which originates from the lower right block of the Jacobian. Evidently, $(J - \lambda^*I)\mathbf{u} = \mathbf{0}$ will give a nontrivial solution with $u_i = 0$, for $i = 1, \ldots 4$, because λ^* is not an eigenvalue of the other two diagonal blocks. In the bottom right block of $J - \lambda^*I$, however, the two rows are linearly dependent. We delete the second one, and are left with the equation $-\lambda^*u_5 + u_6 = 0$, which in terms of our original variables is $-\lambda^*P_3 + Q_3 = 0$, and finally, recalling the definition of Q_3, it becomes the differential equation $P_3' = \lambda^*P_3$. Its solution is therefore $P_3(s) = P_3(0)\exp(\lambda^*s)$. Thus any trajectory leaving from a point near the origin has to lie away from the coordinate hyperplanes, because of the instability of the equilibrium, but it also must remain within the feasible region because biologically we must take the initial condition in this domain, $P_3(0) > 0$.

Because of the upper triangular block structure of the Jacobian, for the equilibria X_1 and X_2 the proof follows the same steps, in turn giving two differential equations whose solutions respectively are $P_1(s) = P_1(0)\exp(\lambda^*s)$ and $P_2(s) = P_2(0)\exp(\lambda^*s)$.

At the equilibria X_3, X_4 and X_5, the positive eigenvalue $\lambda^* > 0$ is a root of a quartic equation stemming therefore from a suitable 4×4 submatrix $\widetilde{J}$ of J. To be specific, let us take the case of X_5.

https://doi.org/10.1051/mmnp/20138605 Published online by Cambridge University Press

The submatrix is the top right 4×4 block of J. If λ^* is an eigenvalue coming from this submatrix, then $P_3 = 0$.

As remarked earlier in Proposition 4.6, the eigenvalues arising from the bottom right block could be of opposite sign, or both negative. In the former case, as argued above, let us take $\lambda_+ > 0$. A sufficient condition for this to occur would be

$$[c(1-\psi_1\psi_2) - \beta K(1-\psi_1) - \delta K(1-\psi_2)]\Delta > 0.$$

We have the equation $P_3' = \lambda_+ P_3$, whose solution is always positive, $P_3(s) = P_3(0)\exp(\lambda_+ s)$, so that the trajectory coming out of the equilibrium remains in the first orthant. If both eigenvalues are negative, $\lambda_\pm < 0$, the same equation shows that P_3 approaches zero with positive values. But the plane $P_1 - P_2$ cannot be crossed because of the existence and uniqueness theorem for ordinary differential equations. The trajectory approaching X_5 will then move away from it along a direction parallel to the $P_1 - P_2$ plane, given by the eigenvector relative to the positive eigenvalue λ^* of the quartic characteristic equation of the submatrix $\widetilde{J}$. Thus, the trajectory coming out of the steady state remains in the feasible region.

The cases for the other two equilibria X_3 and X_4 are treated in a similar way. Note that sufficient conditions for having $\lambda_+ > 0$ in these cases are respectively $\psi_1 c \geq \delta K$, for X_3 and $\psi_1 c \geq \beta K$, for X_4. These combined with the feasibility conditions (4.1) and (4.2) gives possible ranges for the zooplankton mortality to ensure positivity of one eigenvalue

$$\frac{\delta K}{\psi_1} < c < \delta K; \quad \frac{\beta K}{\psi_2} < c < \beta K.$$

□

Therefore we have demonstrated that the necessary conditions of existence of travelling waves are satisfied. They would originate by perturbing anyone of these boundary equilibrium points and progress toward points in the phase space in which all the populations have nonzero values. In particular, they would reach the interior coexistence equilibrium, when the latter is stable.

5. Waves for the toxic model

Now we examine (3.6). In this case the equilibrium $X_3 = (0, P_2, P_3)$ is never feasible, contrary to the former case, while all the other ones present in (3.5) arise here too. As for the other equilibria, we find again the very same points X_0, X_1, X_2, X_4 and X_5. The coexistence point instead is different, in fact a double equilibrium stemming from the roots of a quadratic equation, see [2] for more details.

The Jacobian (4.4) changes only in some elements of the last row of A, which now becomes

$$\left[A_{31}\widetilde{A}_{32}\widetilde{A}_{33}\right] \equiv \left[-\frac{\beta}{D_3}P_3 \quad \frac{\theta}{D_3}P_2P_3\left(\frac{2}{m+P_2} - \frac{P_2}{(m+P_2)^2}\right) \quad \frac{1}{D_3}\left(c - \beta P_1 + \frac{\theta}{m+P_2}P_2^2\right)\right]$$

The main result of this Section parallels the findings of the former one.

Proposition 5.1. *All the equilibria lying on the boundary of the six dimensional phase space are unstable.*

Proof. The origin is unstable, we get the same Jacobian as in the former case.

For X_1, we find $A_{31} = 0$, $\widetilde{A}_{32} = A_{32} = 0$, $\widetilde{A}_{33} = A_{33}$, so that the eigenvalue analysis remains the same.

At X_2 the positive eigenvalue comes from the equation (4.5) which is unchanged, and therefore the instability result still holds.

At X_4 we find $\widetilde{A}_{32} = 0$, $\widetilde{A}_{33} = A_{33} = 0$, and the relevant coefficients of the characteristic equation (4.6), in this case denoted by $\widetilde{a}_i$, coincide with the ones for the non toxic model,

$$\widetilde{a}_1 = a_1 = -\frac{cr_1 v}{D_1 D_3 K\beta} < 0, \quad \widetilde{a}_3 = a_3 = \frac{v}{D_1 D_3}(D_1 + D_3) > 0,$$

https://doi.org/10.1051/mmnp/20138605 Published online by Cambridge University Press

so that again we have at least one positive and one negative eigenvalue.

For X_5 again $\widetilde{A}_{32} = 0$ but $\widetilde{A}_{33} \neq A_{33}$. In the quartic (4.6) there is no change in the two relevant coefficients, namely $\widetilde{a}_1 = a_1$ and $\widetilde{a}_3 = a_3$. Hence the existence of at least one positive and one negative eigenvalue is ensured in this case as well. □

Again, we have shown that all the boundary equilibria in the phase space are unstable, so that the trajectories must remain away from them. We address now the issue that the trajectories must remain in the feasible region.

Proposition 5.2. *The trajectories originating from the unstable boundary equilibria enter into the positive orthant.*

We omit the proof of this result, as it parallels the one of the nontoxic case.

6. Numerical results

In this section we confirm numerically the emergence of the travelling wave solutions studied earlier and investigate further situations that were not covered by the previous theoretical study.

Equations (2.2) are solved by means of a numerical scheme that employs a spatial discretization based on piecewise-linear continuous finite elements and a fully implicit timestepping scheme (Crank-Nicolson). Mass lumping is employed in order to avoid spurious oscillations arising from the reaction terms.

The parameters in the model are set to the same values used in the one dimensional simulations of [2], namely: $\psi_1 = 0.6$, $r_1 = 4.0$, $\alpha_1 = 0.6$, $\psi_2 = 0.8$, $r_2 = 5.0$, $\alpha_2 = 0.7$, $K = 56.0$, for the phytoplanktons and $\beta = 0.4$, $\delta = 0.08$, $c = 3.0$, for the zooplankton in the non-toxic case and $\theta = 0.2$, $m = 5.0$ in the toxic model. For both the non-toxic and the toxic model, simulations are generally performed in the $[0, 100]$ spatial domain. The diffusion coefficients of the zooplankton is set as in [2] to $D_3 = 0.1$. The diffusion coefficients for both phytoplankton species are varied in order to investigate the dependence of the behaviour described here on the relative mobility of the species.

In order to confirm the existence of travelling waves, in each simulation we choose an unstable equilibrium E_r and set the initial value to be $\mathbf{p}(x)|_{t=0} = E_r + \epsilon(x)$ where $\epsilon(x)$ is a local perturbation whose role is to throw the system off equilibrium in a small neighborhood of the left domain boundary. The perturbation $\epsilon(x)$ was always chosen to be nonzero only for one species and in particular for one of the species which is absent in E_r. In this way, all simulations presented in this section have the ecological interpretation of "invasion" by one species of an ecosystem where one or two other species already coexist in a spatially uniform equilibrium. If the solution is a travelling wave with $\mathbf{p}(-\infty) = E_\ell$ and $\mathbf{p}(+\infty) = E_r$, for an equilibrium $E_\ell \neq E_r$, the invasion was successfull and the system moves towards the equilibrium E_ℓ which includes a nonzero density of the new population. If, moreover, the solution of (2.2) with components equal to E_ℓ is spatially homogeneous, at the left of the travelling wave we will observe a "flat" solution corresponding to the new equilibrium of the ecosystem that includes the newly arrived population.

6.1. Existence of travelling waves

In the first set of tests we fixed $D_1 = 1.0$ and $D_2 = 0.5$ as in [2] in order to investigate the existence of travelling waves between different pairs of equilibria. We start from an empty environment (equilibrium E_0) and show that a travelling wave linking E_0 to E_1 exist by setting the initial value to

$$p_1(x) = e^{-x^2} \qquad p_2(x) = 0.0 \qquad p_3(x) = 0.0 \qquad \text{for } x \in [0, 100].$$

The top-left panel of Figure 2 shows a series of snapshots of the solution at increasing times. Of course only the first population is present and it tends to invade the whole domain, leaving behind the equilibrium $E_1 = (56.0, 0.0, 0.0)$. Similarly the top-right panel of Figure 2 shows the travelling wave solution corresponding to the invasion by a second phytoplankton species p_2 of an environment where p_1 is at the

https://doi.org/10.1051/mmnp/20138605 Published online by Cambridge University Press

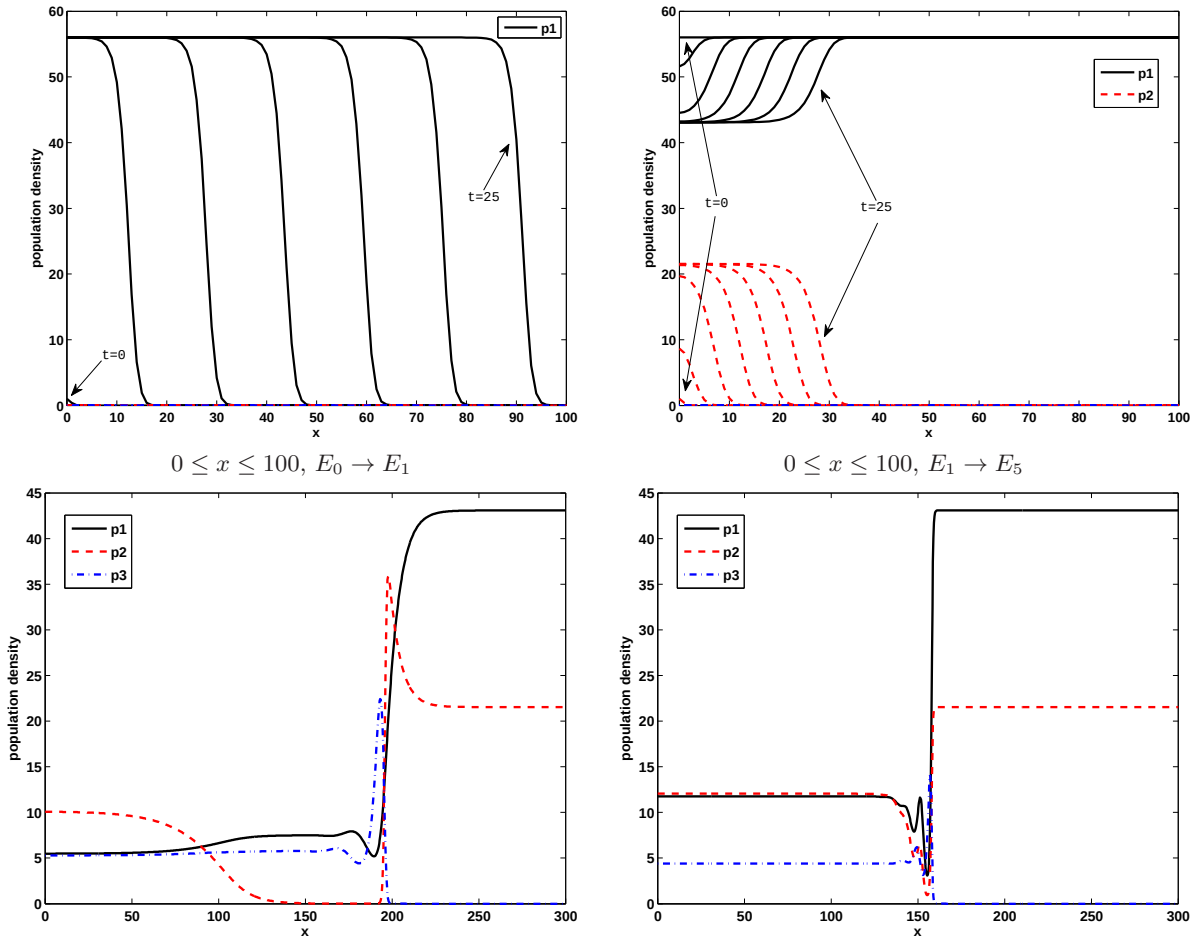


FIGURE 2. Travelling waves between spatially uniform stable equilibria ($D_1 = 1.0, D_2 = 0.5, D_3 = 0.1$). Top: initial value and six snapshots up to $t = 25$ for the invasion of p_1 into an empty environment (right frame) and for the invasion of p_2 into an environment where p_1 is in equilibrium (left frame). Bottom: snapshot at $t = 50$ for the invasion of p_3 into an environment where p_1 and p_2 coexist in equilibrium.

spatially uniform equilibrium E_1. We remark that the speed of this wave is much slower than the previous one. Finally, these two kinds of waves are identical in both the toxic and in the non-toxic models, the third population p_3 is in fact absent and thus no difference arise between the models.

The lower panels of Figure 2 show the transitions between E_5 and E_*. The initial data are

$$p_1(x) = 43.08 \qquad p_2(x) = 21.54 \qquad p_3(x) = e^{-x^2} \qquad \text{for } x \in [0, 100]$$

In this case, the interaction between p_2 and p_3 plays a role and thus the difference between the toxic and non-toxic model is apparent. However, for $D_1 = 1$, the spatially homogeneous internal equilibrium E_* is stable also for the toxic model and thus the travelling wave leaves behind a spatially homogeneous state, namely $(5.47, 10.14, 5.29)$ for the non-toxic model (bottom left in the figure) and $(11.75, 12.05, 4.41)$ for the toxic model (bottom right in the figure). The snapshots shown are taken at $t = 50$ and the computational

https://doi.org/10.1051/mmnp/20138605 Published online by Cambridge University Press

domain has been enlarged to $[0, 300]$ in order to show completely the whole transition, which has a much more complex shape than the previous ones.

6.2. The role of the diffusion coefficient

Next we investigate the transition from E_4 to E_* for both models, varying the diffusion coefficients D_1 and D_2. Initial data were set as a small perturbation of E_4, namely:

$$p_1(x) = 7.50 \qquad p_2(x) = e^{-x^2} \qquad p_3(x) = 5.77 \qquad \text{for } x \in [0, 100] \tag{6.1}$$

The ecological interpretation of this initial condition is the arrival (from the left boundary at $x = 0$) of a second phytoplankton species into an ecosystem where one phytoplankton and the zooplankton population already coexist in equilibrium. In all cases we observe the emergence of a travelling wave solution that represents the invasion of the ecosystem by the new phytoplankton population. The solution has a right-moving front that separates the internal coexistence equilibrium E_* (on its left) and the unstable E_5 equilibrium (on its right). The evolution of the travelling waves is rendered by a sequence of snapshots in Figure 3 for the cases of $D_1 = 1$ (left) and $D_1 = 100$ (right). One can note that the diffusion coefficient does not change the speed of the wave, but it influences the shape of the transition. This is even more evident in Figure 4, where the solutions at $t = 60$ are compared for D_1 ranging from 1 to 10^3. In all four cases the "center" of the transition is located at around $x = 50$, while the width of the transition and the presence of oscillations inside it increases remarkably with the increase of the relative mobility of the species p_1 with respect to the other ones. We also note that changing the value of D_2 does not have significant effects on the shape of the waves.

In the toxic case, the situation is very different, since the initial datum (6.1) represents the arrival in the ecosystem of a phytoplankton species p_2 on which the zooplankton p_3 feeds but which is toxic for p_3. Depending on the value of the diffusion coefficients D_1 and D_2, from [2] it is known when the internal equilibrium is spatially homogeneous. For $D_2 = 0.5$ and $D_3 = 0.1$, the threshold for instability is found at $D_1 = 1.02$, while for $D_1 = 1.0$ and $D_3 = 0.1$, the threshold for instability is found at $D_2 = 0.23$

The left column of Figure 5 shows snapshots of the evolution in the case $D_1 = 1$. In this case, apart from the numerical values of the internal equilibrium, the solution is comparable with the non-toxic case shown in Figure 3. The right column of 5 shows snapshots of the evolution for a value of the diffusion coefficient ($D_1 = 100$) that is above the threshold for instability of the internal equilibrium. This situation is not covered by the theory exposed in the previous sections, but nevertheless we observe a sort of travelling wave, except that at the left of the transition the non spatially uniform equilibrium already observed in [2] emerges.

Figure 6 shows the solutions at $t = 60$ for different values of the diffusion coefficients. For $D_1 = 1$ we observe the appearence of the (stable) spatially uniform internal equilibrium, while for the other cases the solution at the left of the transition is stationary but not spatially uniform. The population densities present oscillations that alternate areas of high concentrations of the toxic species p_2 with high concentrations of the zooplankton p_3. In areas where p_3 is less present, also p_1 has higher concentrations, due to reduced feeding by p_3. Increasing D_1, the wavelength of the spatial oscillations increases. It is remarkable that the mobility of p_1, on its own, can influence the wavelength of the oscillations between the populations p_2 and p_3. The two lower panels of Figure 6 present the case where D_1 is kept at the value used in [2], but D_2 is lowered below the instability threshold. We observe the emergence of another non spatially-uniform equilibrium, with characteristics similar to the ones observed above.

7. Conclusions

We investigate spatially-dependent models of the interaction between two phytoplankton species and one zooplankton population that feeds on the previous two. In particular we consider two cases, distinguished by the toxicity of the second phytoplankton species for the zooplankton. A previous paper [2] had already investigated the stability of spatially uniform equilibria, showing that, when one of the

https://doi.org/10.1051/mmnp/20138605 Published online by Cambridge University Press

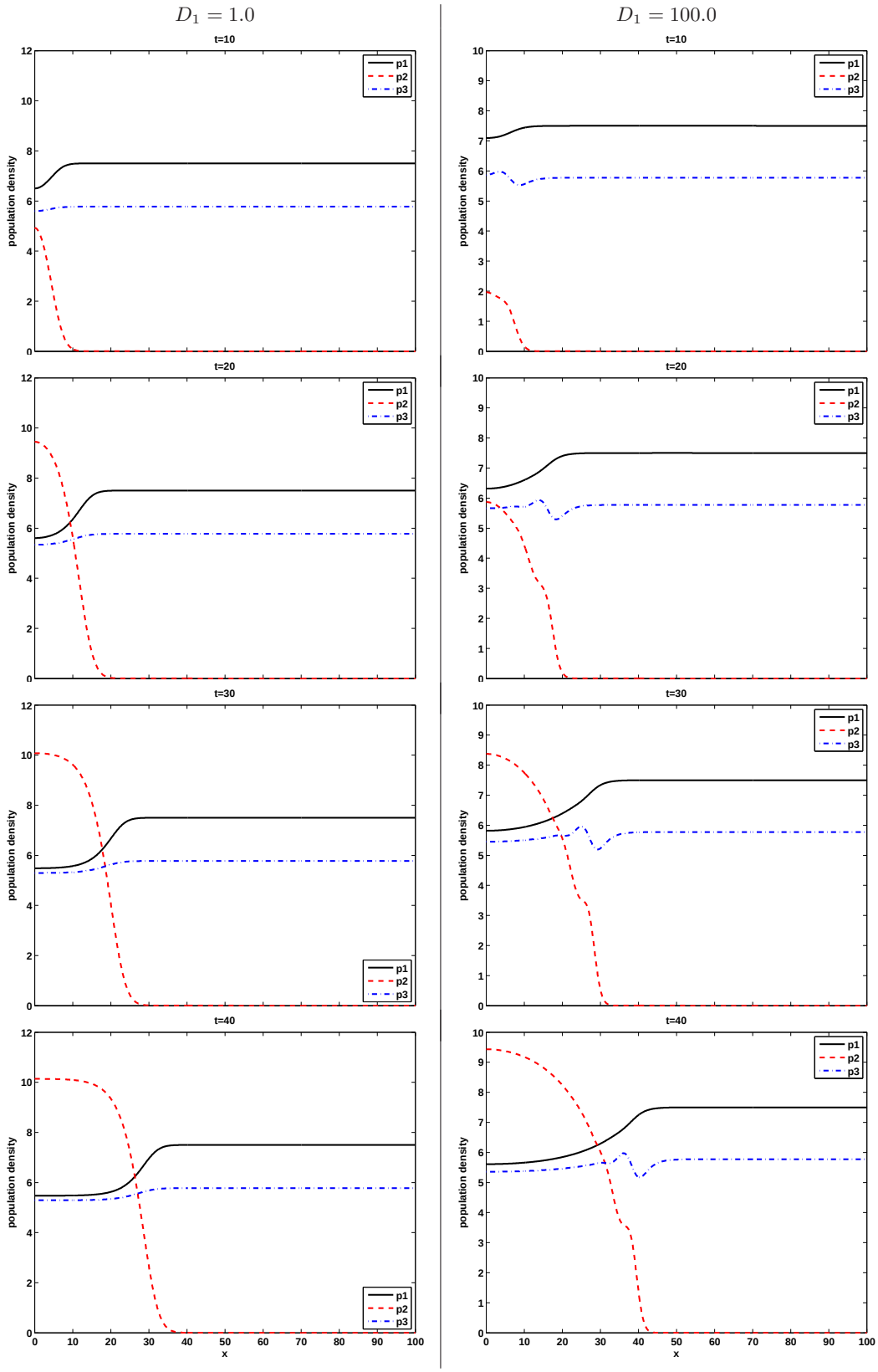


FIGURE 3. Snapshpots for the travelling wave linking E_4 and E_* for the non-toxic model.

https://doi.org/10.1051/mmnp/20138605 Published online by Cambridge University Press

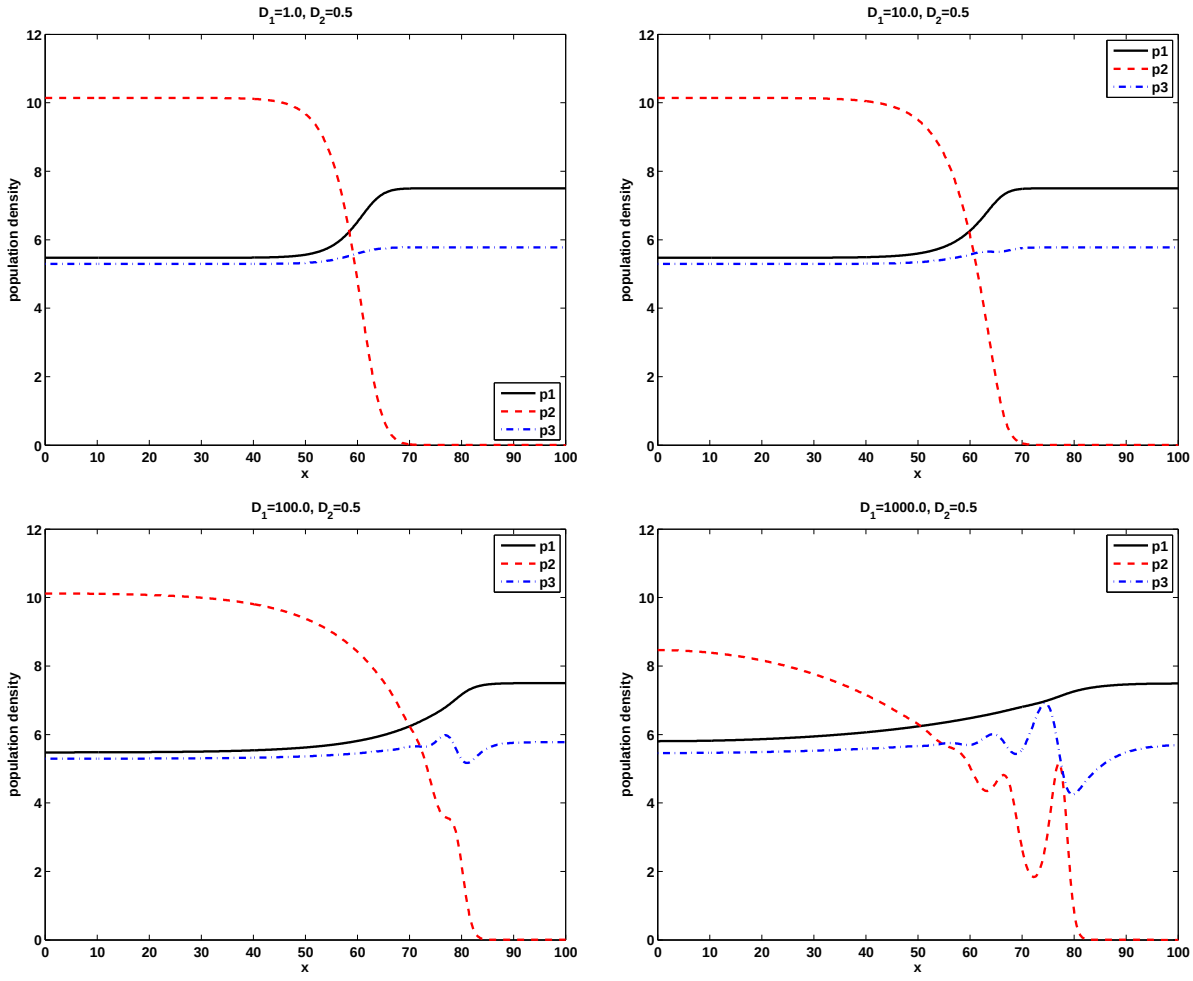


FIGURE 4. Snapshpots at $t = 60$ for the travelling wave linking E_4 and E_* in the non-toxic model.

phytoplankton species is toxic for the zooplankton, the spatially uniform coexistence equilibrium is stable only for moderate values of the relative mobility of the phytoplankton species. This result was confirmed numerically, showing that random initial conditions could lead to the emergence of non spatially-uniform stable equilibria and this result was related to the ecological phenomenon of red tides.

In this paper we consider the more realistic situation in which the system is in equilibrium when a new species appears at a single location in the domain, either due to a point contamination of the environment or coming from a nearby ecosystem. Mathematically, this perturbation throws the system off equilibrium at a single location in space (e.g. on the boundary) and may give rise to an invasion wave. The existence of such travelling waves are investigated both analytically and numerically. The analytical study shows the existence of travelling waves linking pairs of equilibria of the system and is limited to the regimes where spatially uniform equilibria exist. The numerical study confirms the previous findings and additionally investigates the other regime too, showing examples of traveling waves that leave behind them the non spatially-uniform coexistence equilibrium of the toxic model.

https://doi.org/10.1051/mmnp/20138605 Published online by Cambridge University Press

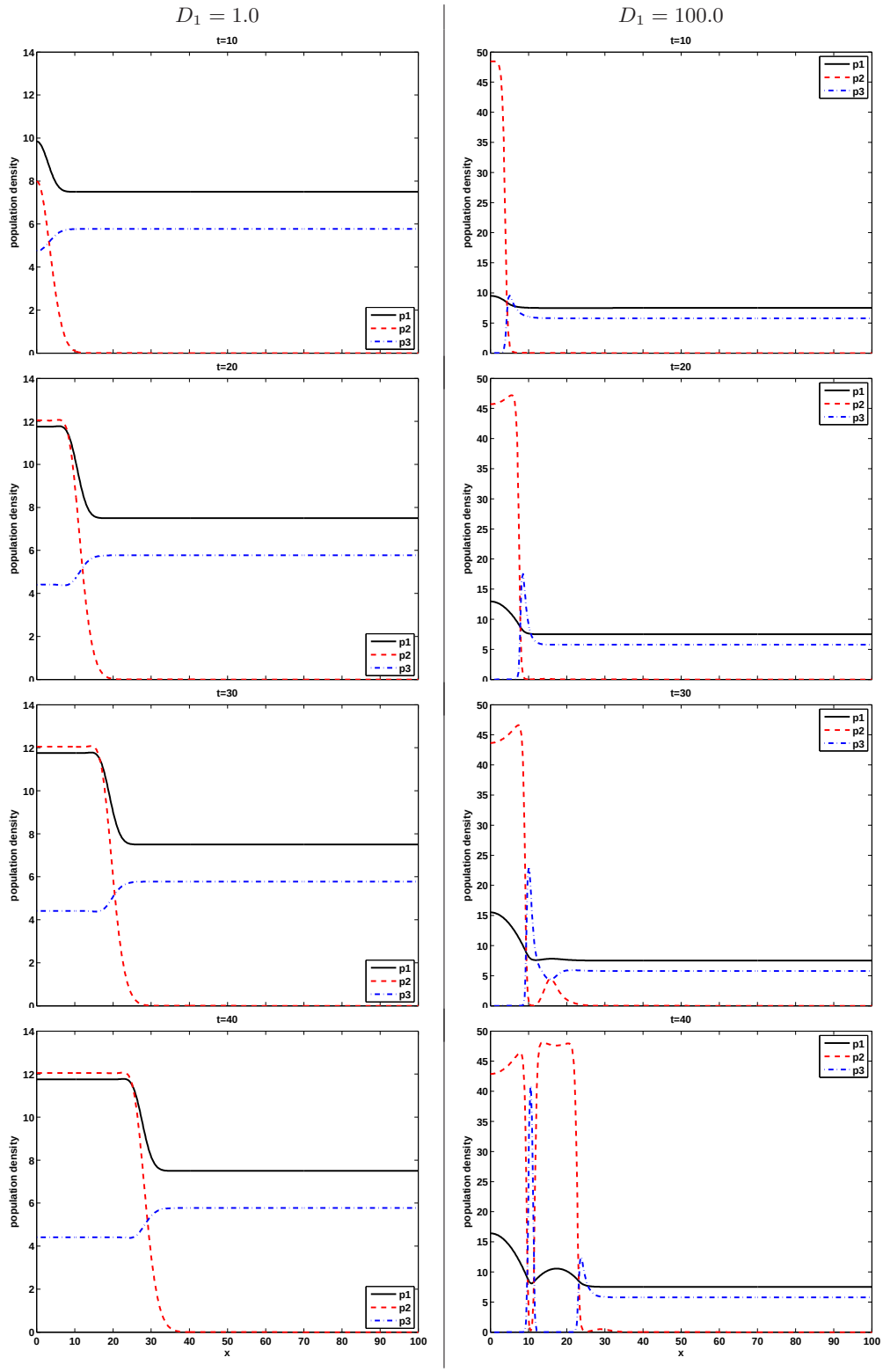


FIGURE 5. Snapshpots for the travelling wave linking E_4 and E_* for the toxic model for $D_2 = 0.5$. Note the different vertical scales.

https://doi.org/10.1051/mmnp/20138605 Published online by Cambridge University Press

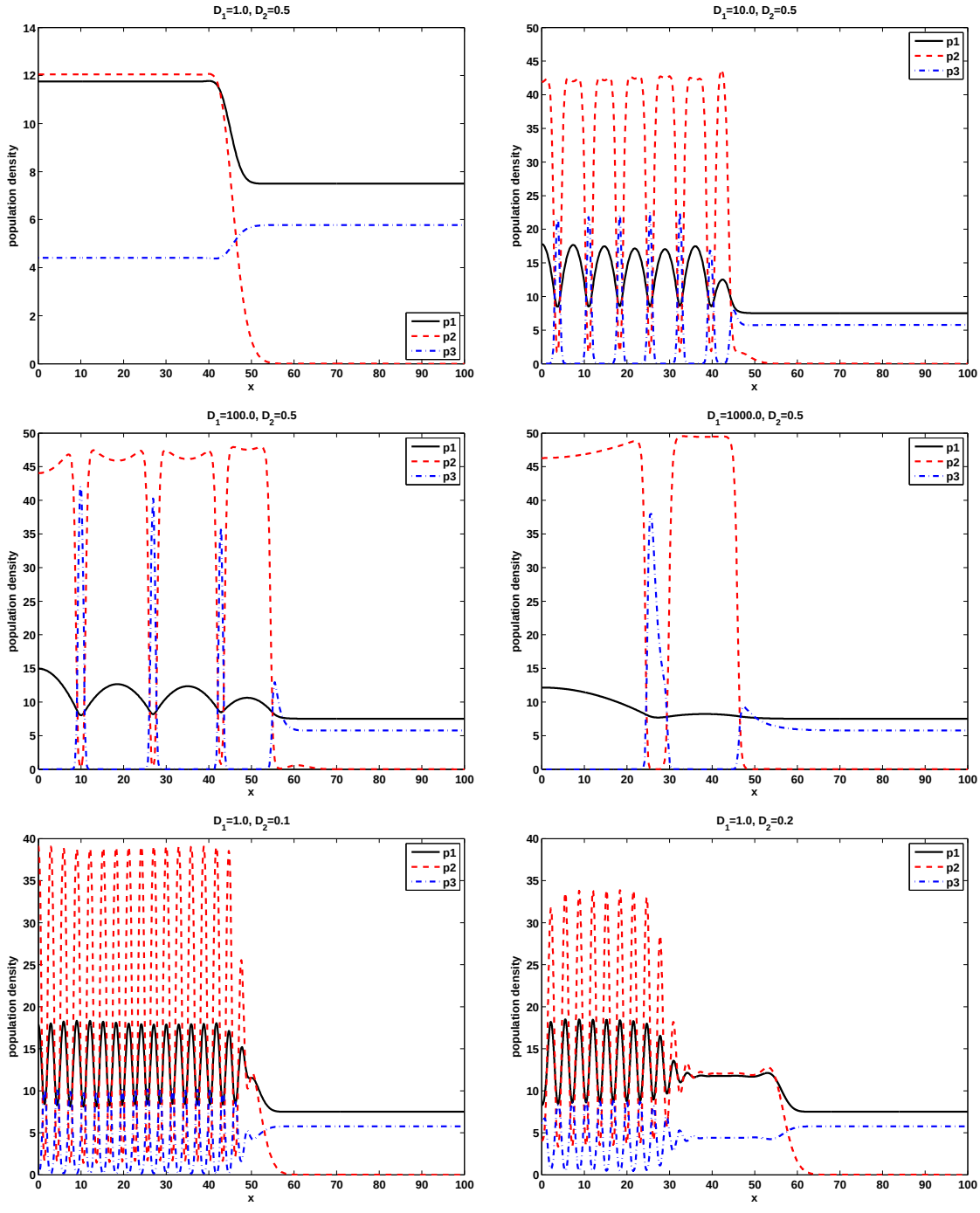


FIGURE 6. Snapshpots at $t = 60$ for the travelling wave linking E_4 and E_* in the toxic model. In the first four panels, D_1 was varied, $D_1 = 1.0$, $D_1 = 10$, $D_1 = 100$, $D_1 = 1000$; in the lower two, D_2 is changed, $D_1 = 1.0$, $D_2 = 0.1$ and $D_1 = 1.0$, $D_2 = 0.2$, .

https://doi.org/10.1051/mmnp/20138605 Published online by Cambridge University Press

References

[1] D. M. L. Anderson. *Toxic algae blooms and red tides: a global perspective*. In Red Tides: Biology, Environmental Science and Toxicology, T. Okaichi, D. M. Anderson, T. Nemoto (Editors). Elsevier: New York, USA (1989), 11–21.

[2] S. Chaudhuri, J. Chattopadhyay, E. Venturino. *Toxic phytoplankton-induced spatiotemporal patterns*. J. Biol. Phys., 38 (2012), 331–348.

[3] S. Chaudhuri, S. Roy, J. Chattopadhyay. *Comparison of plankton dynamics in the 'presence' or 'absence' of toxic phytoplankton*. Appl. Math. Comput., sumbitted for publication.

[4] J. Chattopadhyay, R. R. Sarkar, S. Mandal. *Toxin-producing plankton may act as a biological control for planktonic blooms- field study and mathematical modelling*. J. Theor. Biol., 215, (2002), 333–334.

[5] J. Chattopadhyay, R. R. Sarkar, A. El Abdllaoui. *A delay differential equation model on harmful algal blooms in the presence of toxic substances*. IMA J. Math. Appl. Med. Biol., 19, (2002), 137–161.

[6] G. M. Hallegraeff. *A review of harmful algae blooms and the apparent global increase*. Phycologia, 32, (1993), 79–99.

[7] H. Malchow, S. Petrovskii, E. Venturino. Spatiotemporal patterns in Ecology and Epidemiology. CRC, Boca Raton, 2008.

[8] S. Roy, S. Alam, J. Chattopadhyay. *Competitive effects of toxin-producing phytoplankton on overall plankton populations in the Bay of Bengal*. Bull. Math. Biol., 68(8), (2006), 2303–2320.

[9] S. Roy, S. Bhattacharya, P. Das, J. Chattopadhyay. *Interaction among non-toxic phytoplankton, toxic phytoplankton and zooplankton: inferences from field observations*. J. Biol. Phys., 33(1) (2007), 1–17.

[10] S. Roy. *Spatial interaction among nontoxic phytoplankton, toxic phytoplankton, and zooplankton: emergence in space and time*. J. Biol. Phys., 34, (2008), 459–474.

[11] T. Smayda. *Novel and nuisance phytoplankton blooms in the sea: evidence for a global epidemic*. In Toxic Marine Phytoplankton, E. Graneli, B. Sundstrom, L. Edler, D. M. Anderson (Editors), Elsevier, New York, USA, 1990, 29–40.

https://doi.org/10.1051/mmnp/20138605 Published online by Cambridge University Press